Crystal symmetry and magnetic order in iron pnictides: A tight-binding Wannier function analysis

Z. P. Yin* and W. E. Pickett
Department of Physics, University of California–Davis, Davis, California 95616, USA
(Received 15 December 2009; revised manuscript received 5 May 2010; published 27 May 2010)

To perform a local-orbital analysis of electronic and magnetic interactions, we construct the Wannier functions (WFs) of the Fe $3d$ orbitals in the parent compound of the recently discovered iron-pnictide superconductors, LaFeAsO, and a comparison material LaFePO. Comparing the WFs for the stripe antiferromagnetic order with those for no magnetic order, the difference is a significant spreading (delocalization) of specifically the d_{xy} and d_{xz} (but not d_{yz}) WFs, where parallel Fe spins lie along the x direction. The WF basis gives a tight-binding representation of the first-principles, density-functional based Fe-derived bands. Comparing hopping parameters, it is found that changes due to stripe antiferromagnetism, even if it is weak, enables more isotropic hopping involving spin-majority electrons in the Fe $3d_{xz}$ (but not the $3d_{yz}$) orbital. This change, counterintuitively, actually reinforces electronic anisotropy. Further insight is gained by comparing the WFs of LaFeAsO and LaFePO, identifying how the difference in WFs is related to the difference in hopping integrals and showing how the pnictide atom is influential in forming the stripe antiferromagnetism. Kinetic-energy considerations suggest that orbital fluctuation, in addition to spin fluctuation, may contribute to the decrease in observed ordered moment compared to the calculated values.

DOI: 10.1103/PhysRevB.81.174534 PACS number(s): 74.25.Jb, 74.25.Ha, 74.70.−b

I. BACKGROUND AND MOTIVATION

Since the first report from Hosono's group[1] of superconductivity at $T_c=26$ K in F-doped LaFeAsO, hundreds of experimental and theoretical papers on these iron-pnictide compounds have appeared, aimed at elucidating various properties, including synthesizing new compounds to achieve higher T_c, measuring basic quantities (e.g., magnetic susceptibility, NMR, angle-resolved photoemission spectroscopy), and modeling and simulating to obtain explanations and predictions. Thanks to these efforts, there are now several families of these iron-pnictide superconductors, including the 1111 family (e.g., LaFeAsO and CaFeAsF), 122 family (e.g., $BaFe_2As_2$), 111 family (e.g., LiFeAs), and a more complicated 22426 family (e.g., $Fe_2As_2Sr_4Sc_2O_6$), with T_c up to 56 K.[2] Several aspects have been clarified: the superconductivity lies in primarily iron $3d$ bands[3] and is not phonon mediated;[4] the ground state in most classes is a stripe antiferromagnetic (AFM) phase with a significantly reduced Fe magnetic moment compared to theoretically calculated value;[5,6] it is a moderately correlated system where a Coulomb interaction $U\approx 3$ eV might be appropriate.[7] There is discussion that the superconducting order parameter may have a new $s_{\pm}$ character.[8,9]

Despite a great deal of progress in understanding the electronic structure[10–12] and magnetic interactions,[13–15] some basic questions remain unresolved. One of them is: what is the underlying mechanism of the structural transition from tetragonal to orthorhombic in the parent compounds of iron-based superconductors? This question is especially challenging in the 1111 compounds (e.g., LaFeAsO), where the structural transition is observed (as the temperature is lowered) to occur before[16] the magnetic transition [from nonmagnetic (NM) to stripe antiferromagnetic order which we denote as Q_M AFM]. It would have been natural to think that the stripe antiferromagnetic ordering of Fe provides the driving force for the structural transition because it introduces electronic anisotropy. (Table III in Ref. 17 provides a summary of the structural transition temperature T_S and stripe antiferromagnetic transition temperature T_N of several iron-pnictide compounds.)

Noting that the structural transition and magnetic transition occurs simultaneously in the 122 compounds (e.g., $BaFe_2As_2$), a possible argument is that the magnetism is in fact present, in the form of medium-range order, antiphase boundaries, etc., near the structural transition but its detection is greatly suppressed by strong spatial or temporal fluctuation. The suggestion by Mazin and Johannes that magnetic antiphase boundaries may be the dominant excitation[18] has already stimulated numerical estimations by the present authors.[19] With a time resolution of 10^{-15} s, photoemission experiments by Bondino *et al.*[20] implied a dynamic magnetic moment of Fe with magnitude of $1\mu_B$ in the nonmagnetic phase of $CeFeAsO_{0.89}F_{0.11}$, which is comparable to the ordered magnetic moment of Fe in the undoped antiferromagnetic CeFeAsO compound. The fluctuation strength should be much stronger in 1111 compounds than 122 compounds based on the fact that the measured Fe ordered magnetic moment in 1111 compounds ($\sim 0.4\mu_B$) is much less than in 122 compounds ($\sim 0.9\mu_B$) and they are much smaller than DFT predicted value ($\sim 2\mu_B$).[6,17] One factor is that interlayer coupling of FeAs layers is stronger in 122 compounds than 1111 compounds because the interlayer distance in 122 compounds (~ 6 Å) is significantly smaller than 1111 compounds ($\sim 8-9$ Å).[17] Interlayer interaction should help to stabilize the ordered Fe magnetic moment by reducing fluctuations (reducing two dimensionality).

In this paper we address the effect of magnetic order, and of the pnictide atom, on the strength, character, and spin dependence of Fe-Fe hopping processes by using a Wannier function (WF) representation based on all five Fe $3d$ orbitals, and only these orbitals. Several previous studies of the elec-

tronic structure have pointed out some aspects of the influence of the pnictide, or chalcogenide, atoms (due to size or chemical identities) and also of their positions.[6,21–24] We provide one example of the effect of the pnictogen atom (comparing LaFaAsO with LaFePO) in this paper, where the effect of the pnictogen is included precisely but indirectly through the Wannierization process. This allows us to present results in a Fe-centric picture. This local-orbital representation provides insight into both electronic and magnetic behavior even when the fundamental behavior is primarily itinerant.

II. CALCULATIONAL METHODS

We begin with first-principles calculations using the full-potential local-orbital code[25] (FPLO8) with local-density approximation, exchange-correlation functional[26] (PW92), and the experimental lattice constants and internal atomic coordinates for the compounds LaFeAsO and LaFePO, as given in our previous work.[6,11,19] To obtain a consistent local-orbital representation and the resulting hopping amplitudes, we then construct real-space WFs derived from Fe $3d$ orbitals in both NM and Q_M AFM phases. The WFs used in this paper, as implemented in the FPLO8 code, are constructed by projecting the Bloch functions from a specified energy range onto chosen atomic orbitals, roughly following the method of Ku *et al.*[27,28] The resulting Wannier orbitals retain a symmetry that is common to both the atomic orbital and the point-group symmetry of the site. These WFs provide an explicit basis set of local orbitals that give a tight-binding representation, complete with on-site energies and hopping amplitudes to neighbors as distant as necessary to represent the chosen bands. In this paper we project onto the conventional real Fe $3d$ orbitals with the energy range corresponding to the region with strong Fe $3d$ character in the bands.

III. DIFFERENCES IN BAND STRUCTURES

The differences in electronic structure that we will emphasize result from the changes due to stripe magnetic order, and the differences between LaFeAsO with larger ordered moment, and LaFePO, with smaller calculated moment (experimentally nonmagnetic). The necessary band structures are shown in Fig. 1 for LaFeAsO and Fig. 2 for LaFePO, where in each case the Fe $3d_{yz}$ and Fe $3d_{xz}$ characters are highlighted. The total energy of LaFePO, which is experimentally found to be nonmagnetic, is only slightly lower (2 meV/Fe) in the Q_M AFM phase than the nonmagnetic phase,[11] so the incorrect prediction for LaFePO is actually a fine detail, and suggests it is nearly antiferromagnetic. The calculated Fe magnetic moment of LaFePO in the Q_M AFM phase is $0.52\mu_B$. In LaFeAsO, the calculated moment is near $1.9\mu_B$, substantially larger than the measured value of $0.36\mu_B$ as has been widely discussed (see, for example, Refs. 5 and 11).

For our calculations and discussion we have chosen the x axis along the direction of aligned Fe spins, as shown in Fig. 3; the corresponding zone boundaries are denoted X and Y in the band plots. The nonmagnetic band structures of the two

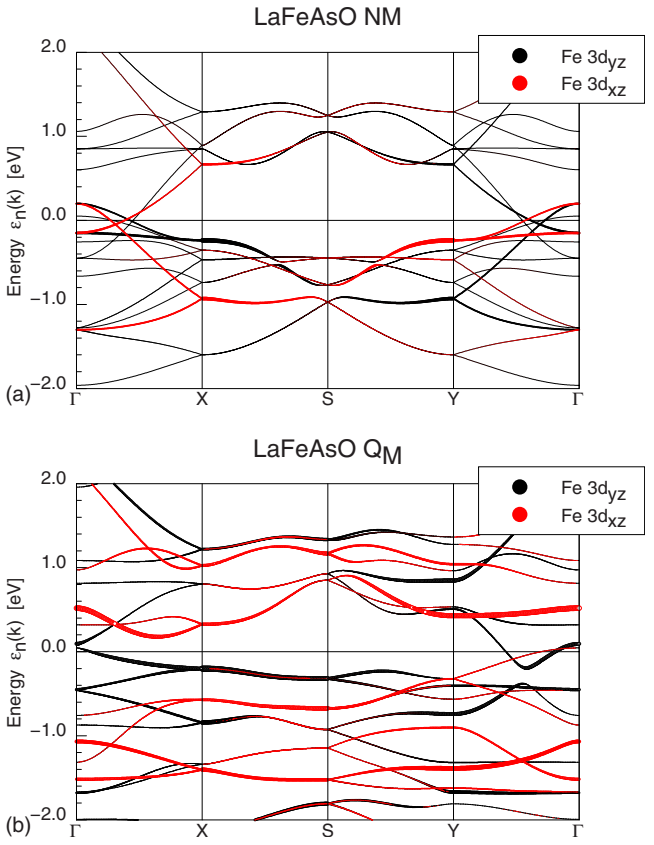

FIG. 1. (Color online) LaFeAsO band structure with highlighted Fe $3d_{yz}$ and Fe $3d_{xz}$ fatband characters in the NM (top panel) and Q_M AFM (bottom panel) phases. Compared to the NM phase, the Fe $3d_{xz}$ bands near Fermi level in the Q_M AFM phase, especially along Γ-X and Γ-Y directions, change dramatically due to the formation of the stripe antiferromagnetism with large ordered Fe magnetic moment of $1.9\mu_B$.

compounds are very similar, differing only in some fine details that do not arise in our analysis. However, the band structures in the Q_M AFM phase of the two compounds differ substantially, which is due to the difference in the Fe magnetic moment ($1.9\mu_B$ vs $0.5\mu_B$).[6,11] The similarities and differences provide a way to study the effect of magnetic order in these compounds, and specifically to show that even small magnetic order has substantial consequences. Since the AFM and NM phases in LaFePO are nearly degenerate, our results have relevance to the effect of (longitudinal) magnetic fluctuations of the Fe atom.

The panels in Fig. 1 illustrate that the magnetic order substantially simplifies the band structure very near the Fermi level, which is all near Γ in this doubled (magnetic) cell. The other difference to notice is the great difference in band structure along Γ-X and Γ-Y directions. Figure 2 shows the influence of a weak stripe antiferromagnetism ($0.5\mu_B$) on the nonmagnetic band structure. The overall band structure remains the same except for some bands near the Fermi energy, where the main change is the separating of the Fe $3d_{xz}$ bands away from the Fermi level, which causes disappearance and change in topology of certain pieces of the Fermi surface of the Fe $3d_{xz}$ bands. Note that the Fe $3d_{yz}$ bands change insignificantly, leaving the bands near the Fermi level

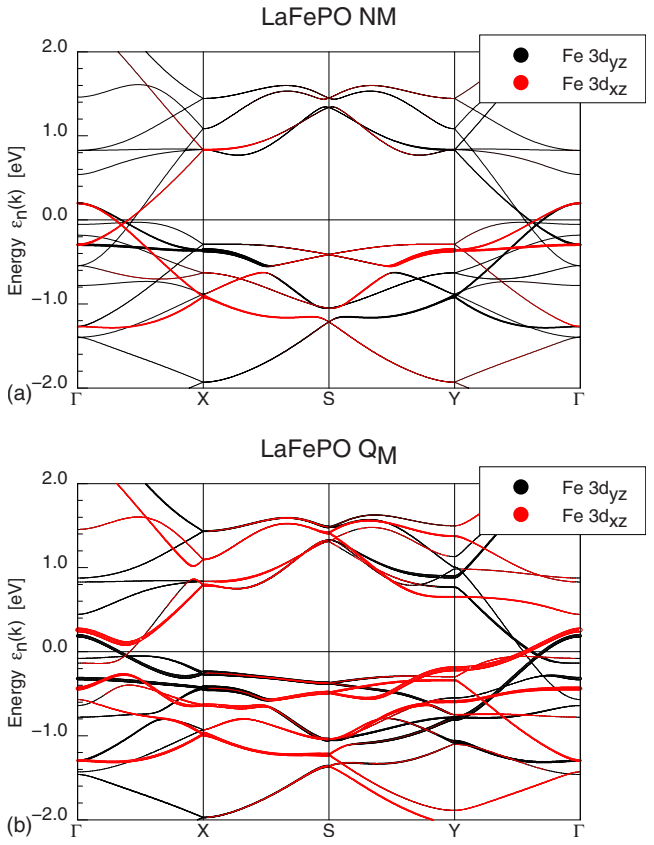

FIG. 2. (Color online) LaFePO band structure with highlighted Fe $3d_{yz}$ and Fe $3d_{xz}$ fatband characters in the NM (top panel) and Q_M AFM (bottom panel) phase. Compared to LaFeAsO, the Fe $3d_{xz}$ bands near Fermi level in the Q_M AFM phase change less significantly from the NM phase, due to the relatively small ordered Fe magnetic moment of $0.5\mu_B$.

dominated by Fe $3d_{yz}$ character. This difference indicates that even a weak stripe antiferromagnetism has a very strong symmetry breaking effect on the $3d_{xz}$ and $3d_{yz}$ bands, which are equivalent in the nonmagnetic state. As a result, even a weak stripe antiferromagnetism induces a large anisotropy, let alone the much stronger (calculated) antiferromagnetism in FeAs-based compounds. (The much bigger anisotropy in the stripe AFM phase in LaFeAsO is evident by comparing Figs. 1 and 2.)

IV. $3d_{xz}$ AND $3d_{yz}$ ORBITAL REPOPULATION

Due to the strong influence of stripe antiferromagnetism on the band structure (even when weak as in LaFePO), the orbital distinction and repopulation of the Fe $3d_{xz}$ and Fe $3d_{yz}$ electrons suggests various means of analysis. The strong intra-atomic anisotropy discussed above is sometimes referred to as orbital ordering, but with the orbital occupations far from integers, the anisotropy also has a substantial itinerant (collective) component. Here we consider briefly the alternative, local viewpoint.

Figure 3 shows two underlying (idealized) orbital populations, both of which are consistent with the Q_M AFM symmetry. (This orbital differentiation is often called "orbital ordering," but based on the calculated populations, discussed below, this is more properly thought of as an itinerant cousin of orbital ordering.) t_{xy} denotes the hopping parameter of the d_{xz}-d_{xz} hopping in the y direction and t_{yx} the d_{yz}-d_{yz} hopping in the x direction. In the nonmagnetic case, by symmetry

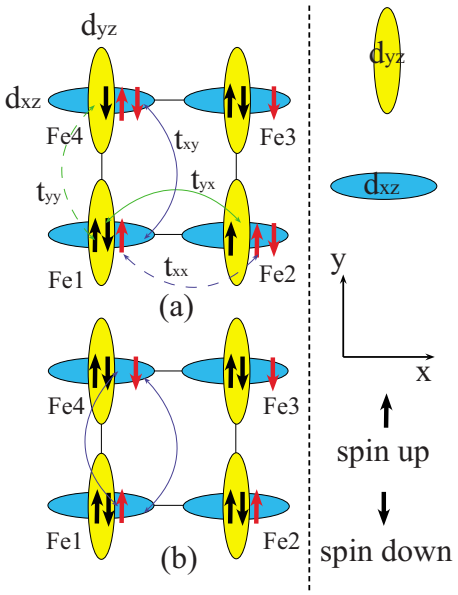

FIG. 3. (Color online) Possible orbital orderings of iron in iron pnictides. Left panel: both (a) and (b) form the Q_M AFM ordering. However, (a) is favored because it gains more kinetic energy from nearest-neighbor hoppings according to second-order perturbation theory (see text). Right panel (from top to bottom) shows the simplified symbols for Fe $3d_{yz}$ and Fe $3d_{xz}$ orbitals, the chosen x and y directions, up arrows for spin-up electrons and down arrows for spin-down electrons, where black arrows (inside the vertical ellipses) for $3d_{yz}$ orbital and red arrows (outside the vertical ellipses) for $3d_{xz}$ orbital.

$$t_{xy} = t_{yx} = t, \tag{1}$$

whereas they differ in the Q_M AFM state. t_{xx} will denote d_{xz}-d_{xz} hopping in the x direction, and similarly t_{yy} denotes d_{yz}-d_{yz} hopping in the y direction (see Fig. 3).

Let U and U' denote the intraorbital and interorbital Coulomb repulsion, and J_H the interorbital Hund's exchange constants. Our purpose is to estimate the difference in kinetic-energy gain of the two configurations shown in Fig. 3. At the level of second-order perturbation theory, the kinetic-energy gain from the d_{yz}-d_{yz} hopping in the x direction [Fig. 3(a)] is

$$\Delta E_{yx} = -t_{yx}^2/(U' - J_H). \tag{2}$$

A similar kinetic gain of

$$\Delta E_{xy} = -t_{xy}^2/(U' - J_H) \tag{3}$$

comes from the d_{xz}-d_{xz} hopping in the y direction [Fig. 3(a)]. t_{xx} and t_{yy} are much smaller and can be neglected (see Table I). Therefore, the total-energy gain from nearest-neighbor (NN) hopping of Fig. 3(a) is

$$\Delta E(a) = \Delta E_{xy} + \Delta E_{yx} = -2t^2/(U' - J_H) \tag{4}$$

while it is

TABLE I. The hopping parameters (in electron volt) of the Fe1 $3d_{yz}$, Fe1 $3d_{xz}$, and Fe1 $3d_{xz}$ orbitals to all the five $3d$ orbitals of its nearest-neighbor Fe2 and Fe4 atoms and next-nearest-neighbor Fe3 atom in the nonmagnetic and Q_M AFM phases of LaFeAsO. The highlighted (italicized and boldface) entries are discussed in the text.

		yz			*xz*			*xy*		
			Q_M			Q_M			Q_M	
Fe1		NM	Up	Dn	NM	Up	Dn	NM	Up	Dn
Fe2	z^2	−0.12	−0.16	−0.08	0	0	0	0	0	0
	x^2-y^2	0.34	0.42	0.28	0	0	0	0	0	0
	yz	−0.33	−0.42	−0.29	0	0	0	0	0	0
	xz	0	0	0	−0.06	**−0.29**	0.09	−0.22	−0.21	−0.20
	xy	0	0	0	−0.22	−0.21	−0.20	**−0.18**	**−0.33**	**−0.07**
Fe4	z^2	0	0	0	−0.12	−0.11	−0.15	0	0	0
	x^2-y^2	0	0	0	−0.34	−0.39	−0.34	0	0	0
	yz	−0.06	−0.09	−0.09	0	0	0	−0.22	−0.21	−0.20
	xz	0	0	0	−0.33	−0.35	−0.35	0	0	0
	xy	−0.22	−0.20	−0.27	0	0	0	−0.18	−0.23	−0.23
Fe3	z^2	−0.10	−0.10	−0.11	−0.10	−0.12	−0.10	−0.17	−0.20	−0.21
	x^2-y^2	0.10	0.09	−0.10	−0.10	−0.09	−0.09	0	0.02	−0.02
	yz	*0.22*	*0.23*	*0.24*	0.08	0.12	0.08	−0.01	0.01	0
	xz	0.08	0.08	0.12	*0.22*	*0.24*	*0.24*	−0.01	−0.02	0.03
	xy	0.01	0	−0.01	0.01	−0.03	0.02	0.13	0.13	0.13

$$\Delta E(b) = -2t^2/U \tag{5}$$

for Fig. 3(b). Because U is larger than $U'-J_H$, the orbital ordering in Fig. 3(a) is favored over Fig. 3(b) by kinetic fluctuations. This result is a more transparent form of an analysis presented by Lee *et al.*[29]

V. TIGHT-BINDING HOPPING PARAMETERS AND WANNIER FUNCTIONS

Figure 4 shows the WFs of all five Fe $3d$ orbitals in both NM and Q_M AFM (majority-spin) phases of LaFeAsO using the same value of isosurface in all cases. In the NM (spin-degenerate, tetragonal) phase, all five WFs for Fe $3d$ orbitals have their density strongly concentrated on the Fe site. All Fe minority-spin $3d$ WFs in the Q_M AFM phase remain almost the same as in the NM phase, so they are not shown. The majority-spin WFs for $3d_{yz}$, $3d_{x^2-y^2}$, and $3d_{z^2}$ orbitals remain very similar to the corresponding Wannier functions in the NM phase, as can be seen in Fig. 4. The significant change is that the majority-spin WFs for $3d_{xz}$ and $3d_{xy}$ become more delocalized in the Q_M AFM phase, with significant density at the NN As sites, the effect being especially large for the d_{xz} orbital. This difference reveals that the majority-spin Fe $3d_{xz}$ and Fe $3d_{xy}$ orbitals mix much more strongly with nearest-neighbor As $4p$ orbitals in the Q_M phase than in the NM phase. The AFM order involves a highly anisotropic magnetization, and resulting difference in majority and minority potentials, that produces this strongly orbital-dependent effect.

Using these WFs as the basis gives a tight-binding representation for which the hopping parameters are obtained from matrix elements of the Wannier Hamiltonian using the FPLO8 code. The corresponding band structures of LaFeAsO and LaFePO are already shown in Figs. 1 and 2 and the resulting tight-binding bands (not shown) fit very well the corresponding density-functional theory (DFT)-local spin density approximation (LSDA) Fe-derived bands in both NM and stripe AFM phases.

Table I presents the hopping parameters of the Fe1 $3d_{yz}$, Fe1 $3d_{xz}$, and Fe1 $3d_{xy}$ orbitals to all the $3d$ orbitals of its nearest-neighbor Fe2 and Fe4 atoms and next-nearest-neighbor Fe3 atom in LaFeAsO. (See Fig. 3 for the definition of each Fe atom.)

The on-site energies (in electron volt) of all the five $3d$ orbitals in the NM phase and Q_M AFM phase in both LaFeAsO and LaFePO are shown in Table II. In the Q_M AFM phase, the on-site energies are shown separately for both spin-up (majority-spin) and spin-down (minority-spin) orbitals. For LaFeAsO, the d_{xz},d_{yz} energies lie at the Fermi level, d_{z^2} and $d_{x^2-y^2}$ lie 0.1–0.3 eV below while d_{xy} lies about 0.2 eV above, without magnetic order. With AFM order, the minority on-site energies do not change greatly, whereas the majority levels fall by 0.7–0.8 eV, thereby affecting the hybridization with the As $4p$ orbitals. The changes in LaFePO are smaller, corresponding to the smaller (factor of ~3) magnetic moments.

The hopping parameters reported here are similar to the corresponding hopping parameters reported by Lee *et al.*[29] and Haule *et al.*[30] (The differences between our results and those of Lee *et al.* reflect the fact that, although the original bands are the same and the Wannier transformation is formally the same, the Wannier transformation is not unique and depends somewhat on some details in the implementation.) Our hopping amplitudes are not directly comparable to

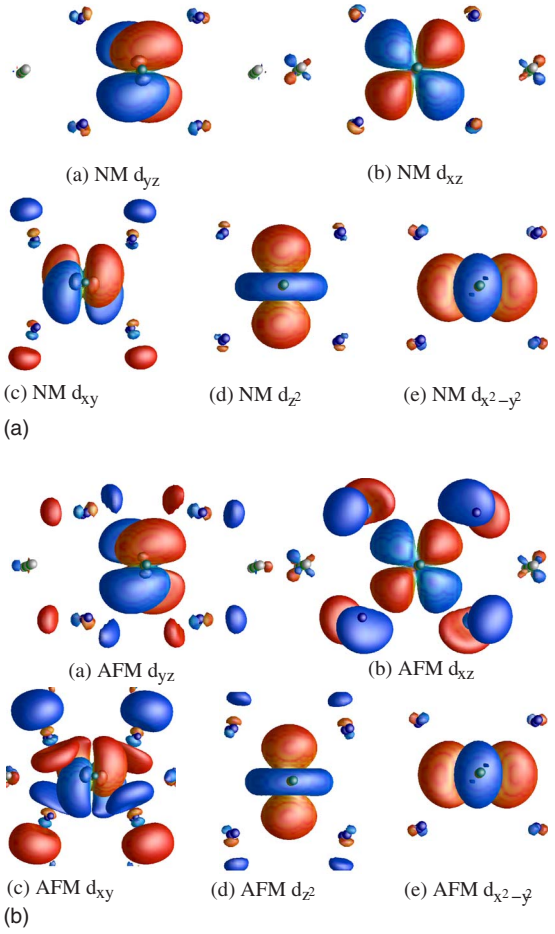

FIG. 4. (Color online) LaFeAsO Wannier functions of Fe $3d$ orbitals in the NM phase (top panel) and those for the majority spin in Q_M AFM phase (bottom panel). The Wannier functions of Fe $3d$ orbitals for the minority spin in the Q_M AFM phase remain almost the same as in the NM phase. The important difference to be observed is that in the Q_M AFM phase, the (majority-spin) Wannier functions of $3d_{xz}$ and $3d_{xy}$ orbitals (and only these) are more extended, with much increased density at neighboring As sites. The isosurface has the same value (density) in each panel.

those reported by Cao *et al.*[31] who focused on the hopping parameters from As $4p$ orbitals to Fe $3d$ orbitals and to its nearest-neighbor As $4p$ orbitals. As shown in Table I, in the NM phase, $t_{xy}=t_{yx}\gg t_{xx}=t_{yy}$, which indicates that the hopping (through As atoms) of d_{xz}-d_{xz}(d_{yz}-d_{yz}) in the $y(x)$ direction of the electrons in Fe $3d_{xz}(3d_{yz})$ orbital is favored over the $x(y)$ direction. The hopping process for Fe $3d_{xz}(3d_{yz})$ electrons is anisotropic. Global tetragonal symmetry is retained because the Fe $3d_{xz}$ and Fe $3d_{yz}$ electrons hop in different directions, which enforces the equivalence of the x and y directions.

In the Q_M AFM phase, the corresponding hopping parameters (both spin up and spin down) are either the same or very close to the NM value, except for two cases. These differences are intimately related to the changes in the corresponding WFs, as we now explain. The first one is the d_{xz}-d_{xz} hopping between parallel spin Fe neighbors (x direction) of a majority-spin electron, whose absolute value increases significantly from the NM case (from −0.06 to −0.29 eV, see the highlighted numbers in Table I). This opens an extra hopping channel in addition to the original d_{xz}-d_{xz} hopping in the y direction. In the NM state, the electrons in the d_{xz} or d_{yz} orbitals separately only hop in one direction (in the sense that the hopping parameters in other directions are relatively small). The dramatic change in the $3d_{xz}$ bands near Fermi level from NM to Q_M AFM, noted in several previous studies, can be traced to this difference.

The other case is for d_{xy}-d_{xy} hopping, again between parallel spin atoms (x direction). In the NM phase, the d_{xy}-d_{xy} hoppings in x and y directions are the same by symmetry, with an amplitude of 0.18 eV. In the Q_M AFM phase, this hopping in the y direction for both spins is slightly enhanced to 0.23 eV. However, the d_{xy}-d_{xy} hopping in the x direction is significantly enhanced to 0.33 for the majority spin and suppressed to 0.07 for the minority spin. These differences shows that the broken symmetry has a strong effect on the d_{xy} orbital's environment.

The magnitude of the changes in the hopping parameters in the two special cases mentioned above, and thus the magnetic order induced changes in WFs, is directly related to the magnitude of the ordered Fe magnetic moment in the Q_M AFM state, which is evident by comparing the case of LaFeAsO and LaFePO (see Tables I and III). The iron atom in the Q_M AFM state in the former compound has a large ordered magnetic moment of $1.9\mu_B$ while in the latter compound it is very weak, only $0.5\mu_B$, in DFT-LSDA calculations. The difference in the ordered Fe magnetic moment is consistent with the change in hopping parameters of d_{xz}-d_{xz}

TABLE II. The on-site energies (in electron volt) of the d_{z^2}, $d_{x^2-y^2}$, d_{yz}, d_{xz}, and d_{xy} Fe orbitals in the NM and Q_M AFM phases in LaFeAsO and LaFePO. In the Q_M AFM phase, the on-site energies are shown separately for the spin-up (majority-spin) and spin-down (minority-spin) orbitals.

	LaFeAsO			LaFePO		
		Q_M			Q_M	
	NM	Up	Dn	NM	Up	Dn
z^2	−0.11	−0.95	0.18	−0.17	−0.35	−0.04
x^2-y^2	−0.27	−1.14	0.07	−0.27	−0.44	−0.14
yz	0.02	−0.67	0.23	−0.04	−0.19	0.07
xz	0.02	−0.70	0.21	−0.04	−0.21	0.07
xy	0.18	−0.50	0.40	0.23	0.13	0.30

TABLE III. The hopping parameters (in electron volt) of the Fe1 $3d_{yz}$, Fe1 $3d_{xz}$, and Fe1 $3d_{xz}$ orbitals to all the five $3d$ orbitals of its nearest-neighbor Fe2 and Fe4 atoms and next-nearest-neighbor Fe3 atom in the nonmagnetic and Q_M AFM phases of LaFePO.

		yz			*xz*			*xy*		
			Q_M			Q_M			Q_M	
Fe1		NM	Up	Dn	NM	Up	Dn	NM	Up	Dn
Fe2	z^2	−0.06	−0.07	−0.05	0	0	0	0	0	0
	x^2-y^2	0.42	0.44	0.41	0	0	0	0	0	0
	yz	−0.37	−0.37	−0.34	0	0	0	0	0	0
	xz	0	0	0	−0.09	**−0.15**	−0.03	−0.23	−0.23	−0.22
	xy	0	0	0	−0.23	−0.23	−0.23	**−0.27**	**−0.31**	**−0.24**
Fe4	z^2	0	0	0	−0.06	−0.06	−0.06	0	0	0
	x^2-y^2	0	0	0	−0.42	−0.43	−0.42	0	0	0
	yz	−0.09	−0.09	−0.09	0	0	0	−0.23	−0.24	−0.22
	xz	0	0	0	−0.36	−0.36	−0.36	0	0	0
	xy	−0.23	−0.22	−0.24	0	0	0	−0.27	−0.27	−0.28
Fe3	z^2	−0.09	−0.08	−0.08	−0.09	−0.09	−0.08	−0.24	−0.24	−0.24
	x^2-y^2	−0.13	0.13	−0.13	−0.13	−0.12	−0.13	0	0	0
	yz	*0.25*	*0.25*	*0.25*	0.09	0.10	0.09	0.04	0.04	0.05
	xz	0.09	0.08	0.10	*0.25*	*0.25*	*0.25*	0.04	0.04	0.05
	xy	−0.04	−0.05	−0.04	−0.04	−0.05	−0.04	0.16	0.16	0.16

and d_{xy}-d_{xy} in the x direction of the spin-majority electron from the NM to the Q_M AFM state, as shown in Tables I and III.

The difference in the changes in the hopping parameters of each Fe $3d$ orbital from NM phase to Q_M AFM phase is related to the spin polarization of each orbital in the Q_M AFM phase, as shown in Table IV. The $3d_{xz}$ orbital has the largest moment ($0.51\mu_B$ in LaFeAsO), followed by the $3d_{xy}$ orbital ($0.48\mu_B$ in LaFeAsO). The other three orbitals have significantly smaller moments (less than $0.41\mu_B$ in LaFeAsO). It is clear that the orbital with larger orbital spin magnetic moment has bigger changes in the relevant hopping parameters. The difference of the relevant hopping parameters between LaFeAsO and LaFePO can also be traced to the difference in the orbital spin magnetic moment.

The transition to the Q_M AFM state is accompanied, in a local picture and to second order, by an extra kinetic-energy gain of

$$\Delta E_{xx} = -t_{xx}^2/(U' - J_H) \tag{6}$$

from the hopping process of d_{xz}-d_{xz} hopping in the x direction, which is comparable with ΔE_{xy}. (Note that ΔE_{xx} is negligible in the NM state.) A substantial extra kinetic-energy gain can also be obtained from the d_{xy}-d_{xy} hopping in the x direction. The anisotropy arises because the majority-spin electron in the $3d_{xz}$ orbital can hop in both directions (i.e., to both parallel and antiparallel spin neighbors) while others in the $3d_{xz}$ and $3d_{yz}$ orbitals can basically only hop in one direction. This anisotropy is reflected in a large symmetry lowering of the $3d_{xy}$ orbital in the AFM phase. The anisotropy leads to a large spin polarization (orbital spin magnetic moment) in the $3d_{xz}$ and $3d_{xy}$ orbital, which may also be related to the tetragonal to orthorhombic structural transition such that the lattice constant along the aligned-spin direction (x direction in this paper) becomes shorter than the other direction (y direction in this paper, thus $a < b$).

TABLE IV. Occupation numbers and spin polarizations in $3d$ orbitals in the NM and Q_M AFM phases of LaFeAsO and LaFePO compounds. δn is the difference of the total occupation number in each orbital between the Q_M AFM phase and the NM phase. m is the spin magnetic moment in each orbital in the Q_M AFM phase.

	LaFeAsO					LaFePO				
			Q_M					Q_M		
	NM	Up	Dn	δn	m	NM	Up	Dn	δn	m
z^2	0.71	0.89	0.48	−0.05	0.41	0.69	0.75	0.64	0.01	0.11
x^2-y^2	0.57	0.80	0.45	0.10	0.34	0.54	0.59	0.50	0.01	0.09
yz	0.65	0.85	0.57	0.11	0.28	0.67	0.72	0.64	0.01	0.08
xz	0.65	0.86	0.35	−0.10	0.51	0.67	0.75	0.56	−0.03	0.19
xy	0.68	0.88	0.39	−0.11	0.48	0.67	0.71	0.62	−0.00	0.09

The additional $3d_{xz}$-$3d_{xz}$ hopping and the enhancement of the $3d_{xy}$-$3d_{xy}$ hoppings, both in the x direction of the spin-majority electron, promote kinetic-energy gain. However, as pictured in Fig. 3(a), the $3d_{xz}$ spin-up electron of Fe1 atom cannot hop in the x direction due to the Pauli principle. In order to take advantage of this extra kinetic-energy gain of ΔE_{xx}, the spin-up occupation number of the $3d_{xz}$ orbital should not be unity but instead must fluctuate. The same situation happens to the $3d_{xy}$ orbital. The competition between the kinetic-energy gain and Pauli principle results in a reduced magnetic moment and is possibly one mechanism of orbital fluctuation.

VI. SUMMARY

In this paper, we have compared the electronic structures of LaFeAsO and LaFePO in both NM and Q_M AFM phases, and find that the stripe antiferromagnetism affects very differently the various Fe $3d$ orbital characters, even when the stripe antiferromagnetism is weak. By comparing LaFeAsO to LaFePO (and looking at similar results for other 1111 and 112 compounds[32,33]), we find that the pnictide atom and the structure are influential in the formation of Q_M AFM phase, consistent with several earlier reports that did not provide any detailed analysis. This information was obtained from a tight-binding representation for Fe $3d$ electrons based on first-principles Wannier functions.

In the nonmagnetic phase the electrons in Fe $3d_{xz}$ and Fe $3d_{yz}$ orbitals have very different amplitudes to hop in the x and y directions, resulting from the positions and chemical character of the pnictide atoms. Anti-intuitively, this "anisotropy" is almost gone for majority-spin electrons in the AFM phase, when the $3d_{xz}$ (or $3d_{yz}$) electron can hop equally to parallel and antiparallel neighbors (both x and y directions). This change is accompanied by a lowering of symmetry, and extension in space, in the $3d_{xy}$ Wannier function. The (large) changes in the near-neighbor hopping parameters of the $3d_{xz}$ and $3d_{xy}$ orbitals in the x direction is directly connected to the much larger orbital spin magnetic moments of these two orbitals than the other three orbitals.

The anisotropy in hopping in the Fe $3d_{yz}$, Fe $3d_{xz}$, and Fe $3d_{xy}$ orbitals also favors orbital fluctuation by providing extra kinetic processes, which are partly compensated by the Pauli principle which inhibits the hopping processes, and which we expect to enhance fluctuations in the corresponding orbital occupation numbers (orbital fluctuation). Such fluctuations would reduce the ordered Fe magnetic moment in the Q_M phase, bringing them closer to the observed ordered moments. On the other hand, interlayer hoppings of the Fe $3d$ electrons in the z direction may help to stabilize the Fe magnetic moment in the Q_M AFM phase.[32,33]

ACKNOWLEDGMENTS

The authors thank Q. Yin and E. R. Ylvisaker for helpful discussions, and K. Koepernik for implementing the calculations of Wannier functions in FPLO code. This work was supported by DOE under Grant No. DE-FG02-04ER46111.

*Present address: Department of Physics and Astronomy, Rutgers University, Piscataway, NJ 08854.

[1] Y. Kamihara, T. Watanabe, M. Hirano, and H. Hosono, J. Am. Chem. Soc. **130**, 3296 (2008).
[2] C. Wang, L. J. Li, S. Chi, Z. W. Zhu, Z. Ren, Y. K. Li, Y. T. Wang, X. Lin, Y. K. Luo, S. Jiang, X. F. Xu, G. H. Cao, and Z. A. Xu, EPL **83**, 67006 (2008).
[3] R. H. Liu, T. Wu, G. Wu, H. Chen, X. F. Wang, Y. L. Xie, J. J. Yin, Y. J. Yan, Q. J. Li, B. C. Shi, W. S. Chu, Z. Y. Wu, and X. H. Chen, Nature (London) **459**, 64 (2009).
[4] L. Boeri, O. V. Dolgov, and A. A. Golubov, Phys. Rev. Lett. **101**, 026403 (2008).
[5] C. de la Cruz, Q. Huang, J. W. Lynn, J. Li, W. Ratcliff, J. L. Zaretsky, H. A. Mook, C. F. Chen, J. L. Luo, N. L. Wang, and P. Dai, Nature (London) **453**, 899 (2008).
[6] Z. P. Yin, S. Lebègue, M. J. Han, B. P. Neal, S. Y. Savrasov, and W. E. Pickett, Phys. Rev. Lett. **101**, 047001 (2008).
[7] M. Aichhorn, L. Pourovskii, V. Vildosola, M. Ferrero, O. Parcollet, T. Miyake, A. Georges, and S. Biermann, Phys. Rev. B **80**, 085101 (2009).
[8] I. I. Mazin, D. J. Singh, M. D. Johannes, and M. H. Du, Phys. Rev. Lett. **101**, 057003 (2008).
[9] Y. Nagai, N. Hayashi, N. Nakai, H. Nakamura, M. Okumura, and M. Machida, New J. Phys. **10**, 103026 (2008).
[10] D. J. Singh and M.-H. Du, Phys. Rev. Lett. **100**, 237003 (2008).
[11] S. Lebègue, Z. P. Yin, and W. E. Pickett, New J. Phys. **11**, 025004 (2009).
[12] I. I. Mazin, M. D. Johannes, L. Boeri, K. Koepernik, and D. J. Singh, Phys. Rev. B **78**, 085104 (2008).
[13] A. N. Yaresko, G.-Q. Liu, V. N. Antonov, and O. K. Andersen, Phys. Rev. B **79**, 144421 (2009).
[14] M. J. Han, Q. Yin, W. E. Pickett, and S. Y. Savrasov, Phys. Rev. Lett. **102**, 107003 (2009).
[15] M. D. Johannes and I. I. Mazin, Phys. Rev. B **79**, 220510(R) (2009).
[16] M. A. McGuire, A. D. Christianson, A. S. Sefat, B. C. Sales, M. D. Lumsden, R. Jin, E. A. Payzant, D. Mandrus, Y. Luan, V. Keppens, V. Varadarajan, J. W. Brill, R. P. Hermann, M. T. Sougrati, F. Grandjean, and G. J. Long, Phys. Rev. B **78**, 094517 (2008).
[17] K. Ishida, Y. Nakai, and H. Hosono, J. Phys. Soc. Jpn. **78**, 062001 (2009).
[18] I. I. Mazin and M. D. Johannes, Nat. Phys. **5**, 141 (2009).
[19] Z. P. Yin and W. E. Pickett, Phys. Rev. B **80**, 144522 (2009).
[20] F. Bondino, E. Magnano, M. Malvestuto, F. Parmigiani, M. A. McGuire, A. S. Sefat, B. C. Sales, R. Jin, D. Mandrus, E. W. Plummer, D. J. Singh, and N. Mannella, Phys. Rev. Lett. **101**, 267001 (2008).
[21] V. Vildosola, L. Pourovskii, R. Arita, S. Biermann, and A. Georges, Phys. Rev. B **78**, 064518 (2008).
[22] K. D. Belashchenko and V. P. Antropov, Phys. Rev. B **78**, 212505 (2008).

[23] T. Yildirim, Phys. Rev. Lett. **102**, 037003 (2009).
[24] M. Berciu, I. Elfimov, and G. A. Sawatzky, Phys. Rev. B **79**, 214507 (2009).
[25] K. Koepernik and H. Eschrig, Phys. Rev. B **59**, 1743 (1999).
[26] J. P. Perdew and Y. Wang, Phys. Rev. B **45**, 13244 (1992).
[27] W. Ku, H. Rosner, W. E. Pickett, and R. T. Scalettar, Phys. Rev. Lett. **89**, 167204 (2002).
[28] W. Ku, H. Rosner, W. E. Pickett, and R. T. Scalettar, J. Solid State Chem. **171**, 329 (2003).
[29] C.-C. Lee, W.-G. Yin, and W. Ku, Phys. Rev. Lett. **103**, 267001 (2009).
[30] K. Haule and G. Kotliar, New J. Phys. **11**, 025021 (2009).
[31] C. Cao, P. J. Hirschfeld, and H.-P. Cheng, Phys. Rev. B **77**, 220506(R) (2008).
[32] See supplementary material at http://link.aps.org/supplemental/10.1103/PhysRevB.81.174534 for results of two other 1111 compounds, two 1111 fluorides, and three 122 compounds.
[33] Z. P. Yin, Ph.D. dissertation, University of California–Davis, 2009.